



# Neutrophil-to-lymphocyte and platelet-to-lymphocyte ratios as predictors of tumor response in hepatocellular carcinoma after DEB-TACE

Isabel Theresa Schobert<sup>1,2</sup> · Lynn Jeanette Savic<sup>1,2</sup> · Julius Chapiro<sup>1</sup> · Khaled Bousabarah<sup>1,3</sup> · Evan Chen<sup>1</sup> · Fabian Laage-Gaupp<sup>1</sup> · Jonathan Tefera<sup>1,2</sup> · Nariman Nezami<sup>1</sup> · MingDe Lin<sup>1</sup> · Jeffrey Pollak<sup>1</sup> · Todd Schlachter<sup>1</sup>

Received: 2 January 2020 / Revised: 15 March 2020 / Accepted: 30 April 2020 / Published online: 19 May 2020  
© European Society of Radiology 2020

## Abstract

**Objectives** To investigate the predictive value of quantifiable imaging and inflammatory biomarkers in patients with hepatocellular carcinoma (HCC) for the clinical outcome after drug-eluting bead transarterial chemoembolization (DEB-TACE) measured as volumetric tumor response and progression-free survival (PFS).

**Methods** This retrospective study included 46 patients with treatment-naïve HCC who received DEB-TACE. Laboratory work-up prior to treatment included complete and differential blood count, liver function, and alpha-fetoprotein levels. Neutrophil-to-lymphocyte ratio (NLR) and platelet-to-lymphocyte ratio (PLR) were correlated with radiomic features extracted from pretreatment contrast-enhanced magnetic resonance imaging (MRI) and with tumor response according to quantitative European Association for the Study of the Liver (qEASL) criteria and progression-free survival (PFS) after DEB-TACE. Radiomic features included single nodular tumor growth measured as sphericity, dynamic contrast uptake behavior, arterial hyperenhancement, and homogeneity of contrast uptake. Statistics included univariate and multivariate linear regression, Cox regression, and Kaplan–Meier analysis.

**Results** Accounting for laboratory and clinical parameters, high baseline NLR and PLR were predictive of poorer tumor response ( $p = 0.014$  and  $p = 0.004$ ) and shorter PFS ( $p = 0.002$  and  $p < 0.001$ ). When compared to baseline imaging, high NLR and PLR correlated with non-spherical tumor growth ( $p = 0.001$  and  $p < 0.001$ ).

**Conclusions** This study establishes the prognostic value of quantitative inflammatory biomarkers associated with aggressive non-spherical tumor growth and predictive of poorer tumor response and shorter PFS after DEB-TACE.

## Key Points

- In treatment-naïve hepatocellular carcinoma (HCC), high baseline platelet-to-lymphocyte ratio (PLR) and neutrophil-to-lymphocyte ratio (NLR) are associated with non-nodular tumor growth measured as low tumor sphericity.
- High PLR and NLR are predictive of poorer volumetric enhancement-based tumor response and PFS after DEB-TACE in HCC.
- This set of readily available, quantitative immunologic biomarkers can easily be implemented in clinical guidelines providing a paradigm to guide and monitor the personalized application of loco-regional therapies in HCC.

**Keywords** Hepatocellular carcinoma · Platelet count · Neutrophils · Lymphocytes · Radiomics

---

Isabel Schobert and Lynn Jeanette Savic contributed equally to this work.

**Electronic supplementary material** The online version of this article (<https://doi.org/10.1007/s00330-020-06931-5>) contains supplementary material, which is available to authorized users.

---

✉ Julius Chapiro  
julius.chapiro@yale.edu

<sup>1</sup> Department of Radiology and Biomedical Imaging, Yale School of Medicine, 300 Cedar Street, New Haven, CT 06520, USA

<sup>2</sup> Institute of Radiology, Charité - Universitätsmedizin Berlin, corporate member of Freie Universität Berlin, Humboldt-Universität, and Berlin Institute of Health, 10117 Berlin, Germany

<sup>3</sup> Department of Stereotactic and Functional Neurosurgery, University Hospital of Cologne, Cologne, Germany

## Abbreviations and acronyms

AFP	Alpha-fetoprotein
ALC	Absolute lymphocyte count
ALT	Alanine aminotransferase
ANC	Absolute neutrophil count
AP	Alkaline phosphatase
AST	Aspartate aminotransferase
BCLC	Barcelona Clinic Liver Cancer
DEB	Drug-eluting bead
ETB	Enhancing tumor burden
HCC	Hepatocellular carcinoma
HIPAA	Health Insurance Portability and Accountability Act
LI-RADS	Liver Imaging Reporting and Data System
NLR	Neutrophil-to-lymphocyte ratio
PFS	Progression-free survival
PLR	Platelet-to-lymphocyte ratio
qEASL	Quantitative European Association for the Study of the Liver
TACE	Transarterial chemoembolization
TB	Tumor burden
TME	Tumor microenvironment
TTV	Total tumor volume
VEGF	Vascular endothelial growth factor

## Introduction

Hepatocellular carcinoma (HCC) is the sixth most common cancer with continuously increasing incidence rates worldwide [1]. The majority of patients with HCC are diagnosed at intermediate to advanced disease stages and are thus no longer amenable to curative therapies [2]. In this setting, intra-arterial therapies, such as transarterial chemoembolization (TACE), are guideline-approved treatments [3, 4]. The Barcelona Clinic Liver Cancer (BCLC) classification is currently endorsed as the standard system for the management of HCC by leading cancer society guidelines, e.g., the European Association for the Study of Liver [5, 6]. BCLC criteria inform treatment decisions and estimate prognosis based on tumor manifestation, performance status, and liver function [7, 8]. However, one of the main limitations of the BCLC system involves treatment indication for TACE in the intermediate stage (B), which includes a considerably heterogeneous patient population with varying degrees of tumor extension, liver functional reserve, and disease etiology, that results in heterogeneous therapeutic efficacy within the same BCLC stage [9].

One of the reasons why BCLC stages comprise a heterogeneous patient population may be the manual assessment of tumor manifestation, which is limited to unidimensional measurements or a qualitative nature [10]. Thus, there is a clinical need to identify image analysis strategies with high accuracy

and robust diagnostic performance in order to overcome those limitations. In this context, radiomic feature analysis has recently been introduced to enable automated, objective, and quantitative lesion characterization derived from a pixel-by-pixel analysis [11].

In addition to imaging features, the complex and adaptive nature of HCC and its interplay with the tumor microenvironment (TME) cause a high degree of heterogeneity between tumors and potentially play a critical role in susceptibility of cancer cells to nonsurgical therapies including TACE [12]. Specifically, chronic liver diseases are hypothesized to generate a pro-inflammatory environment allowing for hepatic tumor formation and progression [12–15]. While tumor-infiltrating lymphocytes are part of the anti-tumoral inflammatory response, neutrophils and high platelet count suppress anti-tumoral immune cell function and promote neoangiogenesis by secretion of vascular endothelial growth factor (VEGF) [16, 17]. Thus, inflammatory ratios such as neutrophil-to-lymphocyte (NLR) and platelet-to-lymphocyte (PLR) can potentially serve as quantitative biomarkers for individual tumor characterization that have been linked with tumor angiogenesis, immune evasion, and metastatic disease [18, 19].

Therefore, this study aimed to assess the correlation of quantifiable imaging and inflammatory features and to elucidate their prognostic value for the clinical outcome in HCC after drug-eluting bead (DEB)-TACE measured as volumetric tumor response and progression-free survival (PFS).

## Material and methods

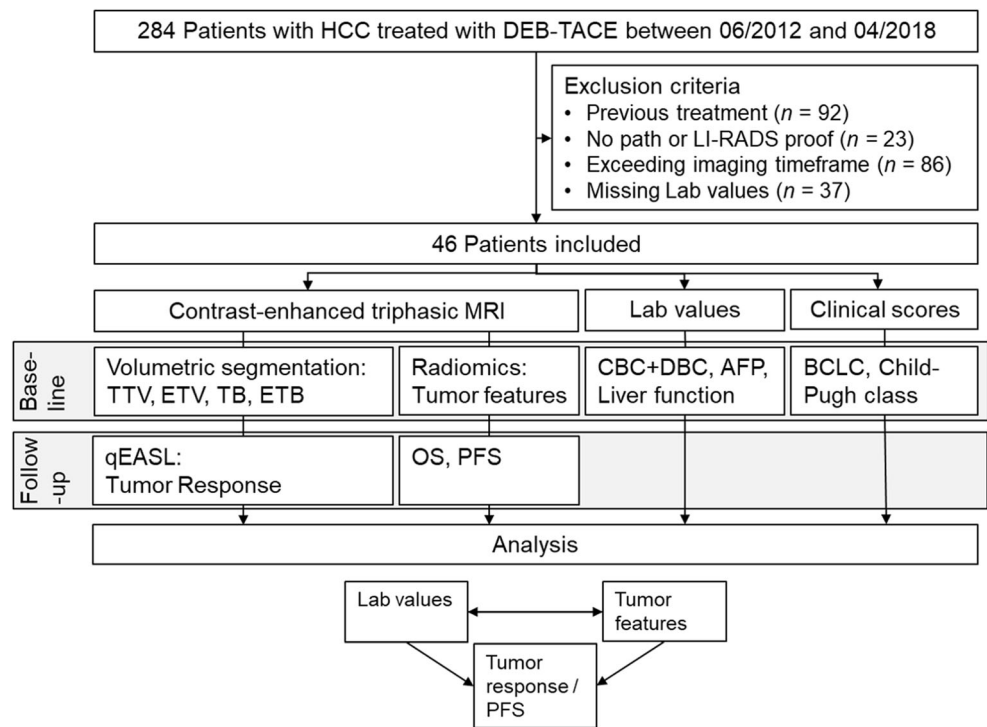
### Study cohort

This Health Insurance Portability and Accountability Act of 1996 (HIPAA)-compliant, retrospective study was approved by the Institutional Review Board. Informed consent was waived. All tumors included in the analysis were histopathologically proven to be HCC or diagnosed using Liver Imaging Reporting and Data System v2018 (LI-RADS; [20]). Baseline contrast-enhanced MRI had to be within 4 months prior to treatment, and the first follow-up contrast-enhanced MRI had to be within 3 months after treatment for patients to be included. In total, 46 patients with 50 treatment-naïve HCC, who received DEB-TACE between 2012 and 2018, were included. Figure 1 illustrates the patient selection process and methodological workflow.

### Drug-eluting bead TACE procedure

Patients were treated with DEB-TACE using bead sizes of 40–90  $\mu\text{m}$  ( $n = 1$ ), 70–150  $\mu\text{m}$  ( $n = 25$ ), 100–300  $\mu\text{m}$  ( $n = 18$ ), and 300–500  $\mu\text{m}$  ( $n = 2$ ) (LC Bead, Boston Scientific).

**Fig. 1** Study workflow and exclusion criteria. AFP, alpha-fetoprotein; BCLC, Barcelona Clinic Liver Cancer; BL, base-line; CBC, complete blood count; DBC, differential blood count; DEB-TACE, drug-eluting bead transarterial chemoembolization; ETB, enhancing tumor burden; ETV, enhancing tumor volume; F/U, follow-up; HCC, hepatocellular carcinoma; LI-RADS, Liver Imaging Reporting and Data System; OS, overall survival; PFS, progression-free survival; TB, tumor burden; TTV, total tumor volume; qEASL, quantitative European Association for the Study of the Liver



For the treatment, trans-femoral access was gained, and a catheter was advanced into the coeliac axis for digital subtraction angiography. Then, a microcatheter was placed into a segmental or subsegmental hepatic artery branch for administration of up to 4 mL of DEBs (loaded with 25 to 37.5 mg of doxorubicin per mL beads).

**Laboratory values**

Laboratory reports from all patients within 2 months prior to DEB-TACE were reviewed for complete and differential blood counts, alpha-fetoprotein, and liver function tests. Platelet count, absolute neutrophil count (ANC), absolute lymphocyte count (ALC), NLR, PLR, alpha-fetoprotein (AFP), alkaline phosphatase (AP), aspartate aminotransferase (AST), alanine aminotransferase (ALT), and bilirubin were included in the analysis. For Kaplan–Meier analysis, NLR and PLR were divided into low and high values according to the mean NLR and PLR within the study cohort.

**Magnetic resonance imaging acquisition**

All patients received MR imaging of the liver before (median, 1.44; range, 0.06–3.56 months) and 1 month (median, 1.21; range, 0.72–2.33 months) after DEB-TACE. Scans were acquired according to the standardized institutional protocol. Briefly, MRI was performed on a 1.5-T MR unit (Magnetom Avanto; Siemens) using a phased-array torso coil.

The protocol included breath-hold unenhanced and contrast-enhanced (0.1 mmol/kg intravenous Dotarem; Guerbet) T1-weighted imaging in the hepatic arterial, portal venous, and delayed phase (20, 70, and 180 s after contrast administration).

**MR image data analysis**

**Volumetric image analysis**

Up to two dominant tumors were determined on baseline imaging as the largest lesions and included in the analysis. Included tumors were required to be pathologically proven or meet LI-RADS criteria. The dominant tumors were volumetrically segmented on the arterial-phase T1-weighted baseline and follow-up MRI and total tumor volume (TTV) was calculated.

The software-based 3D “quantitative European Association for the Study of the Liver” (qEASL) tool (IntelliSpace Portal, version 8, Philips Healthcare) was used to calculate the enhancing tumor volume (ETV in cm<sup>3</sup>) prior to treatment as previously described [21]. In addition, the entire liver was segmented and the total (TB) and enhancing tumor burden (ETB) were assessed.

In order to assess volumetric tumor response, changes of the enhancing tumor diameter and ETV between baseline and follow-up imaging were calculated and interpreted according to the established response criteria including modified Response Evaluation Criteria In Solid Tumors (mRECIST)

and qEASL criteria. Response was categorized as complete and partial response, stable, and progressive disease, objective and nonobjective response (OR, non-OR) [21].

### Quantitative radiomics approach based on tumor morphology and histogram analysis

Tumor features extracted in Python 3.6.5 (Python Software Foundation) using the open-source package Pyradiomics were used to describe macroscopic appearance of lesions [22]. First-order statistics based on the distribution of voxel intensities contained in the delineated tumor masks were calculated for all multiphase MRI scans. Additionally, features descriptive of the tumor shape were used. For the sake of clinical interpretability, features of higher order were not employed. Clinically useful and comprehensible imaging features that represent pathophysiological tumor characteristics were chosen for further analysis and these are tumor sphericity as an indicator of single nodular tumor growth, difference between the mean gray levels of the noncontrast and arterial phase as arterial hyperenhancement, difference between the mean gray levels of the arterial and venous phase as contrast enhancement dynamics, arterial kurtosis indicative of a necrotic core, and arterial variance reflecting inhomogeneous contrast uptake behavior.

### Statistical analysis

Descriptive results are reported as absolute and relative frequency ( $n$  and %), mean and standard deviation (SD), or median and range.

To assess independent predictors of tumor response to DEB-TACE, a three-step approach was used including univariable and multivariable linear regression. First, parameters that correlated with response to DEB-TACE in the univariate analysis ( $p$  value  $\leq 0.1$ ) were amenable for inclusion in the multivariable linear regression model. Second, to avoid overfitting of the multivariable linear regression model, variables were further limited up to a maximum of four covariates based on the total number of included patients being  $n = 46$ . This selection of variables was performed according to an established stepwise forward selection algorithm [23]. Ultimately, only the variables with the strongest effect on the outcome were included into the multivariable regression model. As NLR and PLR both take into account lymphocyte count, two separate multivariable linear regression models were created for NLR and PLR, respectively [23].

For the correlation of baseline tumor imaging features with immunologic ratios, a linear regression model was used.

Overall and progression-free survival (OS and PFS) were measured. Overall survival was defined as the time from initial treatment using DEB-TACE to the date of death. PFS was used for analysis. Survival analysis comprised multivariable

Cox regression reported as hazard ratio and 95% confidence interval (CI) and subsequent Kaplan–Meier analysis using log-rank testing. Two separate models were created for NLR and PLR, applying TB and Child–Pugh class as covariates, as they are considered clinically relevant influencing factors for PFS [24, 25].

A two-sided  $p$  value  $< 0.05$  was considered statistically significant. Statistical analyses were performed using SPSS (v25.0, IBM Corp.) and GraphPad Prism (v7.00).

**Table 1** Baseline patient characteristics

Demographics	<i>N</i> (%)
Patient characteristics	
Number of patients	46 (100)
Age (years), mean $\pm$ SD	64.44 $\pm$ 9.66
Male/female	37/9 (80.43/19.57)
Ethnicity	
Caucasian	31 (67.39)
African-American	8 (17.39)
Hispanic	5 (10.87)
Asian	2 (4.35)
Disease characteristics	
HCC proof	
Biopsy/explant	15 (32.61)
LI-RADS	31 (67.39)
Etiology of cirrhosis	
Hepatitis B	2 (4.35)
Hepatitis C	18 (39.13)
Alcoholic steatohepatitis	18 (39.13)
Nonalcoholic steatohepatitis	7 (15.22)
Unknown	1 (2.17)
Child–Pugh class	
A	28 (60.87)
B	15 (32.61)
C	3 (6.52)
Eastern Cooperative Oncology Group performance status	
0	31 (67.39)
$\geq 1$	10 (21.74)
Unknown	5 (10.87)
Barcelona Clinic Liver Cancer stage	
A	8 (17.39)
B	14 (30.43)
C	6 (13.04)
N/A	18 (39.13)
Unifocal/multifocal	16 (34.78)/30 (65.22)
Tumor diameter, mean $\pm$ SD	3.83 $\pm$ 2.09
Main portal vein thrombosis	6 (13.04)

HCC, hepatocellular carcinoma; LI-RADS, Liver Imaging Reporting and Data System; SD, standard deviation

## Results

### Study population

The baseline characteristics of the patient population are presented in Table 1. Briefly, the study population comprised 37 males (80.43%) and 9 females (19.57%) with a mean age of  $64.44 \pm 9.66$  years. Of 50 included tumors, 15 were pathologically proven (32.61%) and 31 tumors met LI-RADS v2018 criteria (67.39%). Median follow-up time was 12.52 months (range 0.97–46.24).

Descriptive results of the baseline laboratory values are displayed in Supplemental Table 1 and descriptive results of the quantitative image analysis are shown in Supplemental Table 2. Tumor response rates according to mRECIST and qEASL are displayed in Supplemental Table 3. Correlation of baseline laboratory values with baseline tumor features is displayed in Supplemental Table 4. After the follow-up imaging, which was used for response assessment, 16 patients (34.78%) received TACE, 6 patients (13.04%) received radiofrequency ablation, 5 patients (10.87%) underwent liver transplant, and 1 patient (2.17%) received radioembolization with yttrium-90.

Regarding OS, 14 patients died and 32 were censored. As 32 patients were censored, median OS was undefined. Progression-free survival was defined as the time from initial DEB-TACE to the date of death or progression by means of mRECIST. According to institutional standard operating procedures, follow-up imaging was obtained every 2–3 months. At the end of follow-up (November 2018), 22 (47.83%) patients had tumor progression and 7 (15.22%) had died. A total of 19 (41.3%) patients were censored. Of those 19 patients, 7 were lost to follow-up, 4 were still alive without tumor recurrence, 3 had undergone liver transplant, 3 had loco-regional treatments of the index tumor, and 2 had another TACE of the index tumor. Median PFS was 12.77 months. According to the Kaplan–Meier curve, 1-year PFS was 53.346%, 2-year PFS was 27.661%, and 3-year PFS was 27.661%.

### Correlation of laboratory biomarkers, baseline tumor imaging features, and tumor response after DEB-TACE

Regarding volumetric and enhancement-based tumor characteristics, AFP correlated with TB and ETB ( $p = 0.001$  and  $p < 0.001$ ). As for the immunologic laboratory values, ANC correlated with TB but not with ETB ( $p = 0.003$  and  $p = 0.1$ ). NLR and PLR did not correlate with TB ( $p = 0.102$  and  $p = 0.249$ ) or ETB ( $p = 0.771$  and  $p = 0.858$ ).

However, a linear regression of shape-based sphericity with immunologic markers revealed that NLR and PLR correlated inversely with sphericity ( $R^2 = 0.230$  and  $p = 0.001$ ,  $R^2 = 0.271$  and  $p < 0.001$ , respectively). Specifically, tumors with a high level of sphericity indicating single nodular tumor growth revealed lower NLR and PLR than nonspherical tumors (Figs. 2 and 4). Arterial hyperenhancement ( $p = 0.144$  and  $p = 0.337$ ), contrast enhancement dynamics ( $p = 0.59$  and  $p = 0.988$ ), arterial kurtosis ( $p = 0.703$  and  $p = 0.812$ ), and heterogeneity of contrast uptake ( $p = 0.937$  and  $p = 0.843$ ) did not show significant correlations with NLR and PLR.

The baseline tumor imaging features TTV, ETV, TB, and ETB were tested regarding differences in OR and non-OR and the results are displayed in Table 2.

### Correlation of baseline immunologic markers and tumor response after DEB-TACE

Baseline laboratory and patient-related parameters were compared regarding OR and non-OR in Table 2. NLR and PLR distribution in each response category was compared in Table 3. In the present cohort, NLR and PLR were both associated with tumor response in a univariable linear regression model ( $p = 0.004$  and  $p = 0.001$ ) (Figs. 3 and 4). After adjusting for TB, Child–Pugh class, and AP in the multivariable linear regression analysis, high NLR ( $p = 0.014$ ,  $R^2 = 0.616$ ) and PLR ( $p = 0.004$ ,  $R^2 = 0.639$ ) were still

**Fig. 2** Linear regression of tumor sphericity on baseline imaging and inflammatory markers prior to treatment. This graph demonstrates that more single nodular growth patterns of tumors, measured as increased tumor sphericity, correlate with low (a) neutrophil-to-lymphocyte ratio (NLR) ( $p = 0.001$ ) and (b) platelet-to-lymphocyte ratio (PLR) ( $p < 0.001$ )

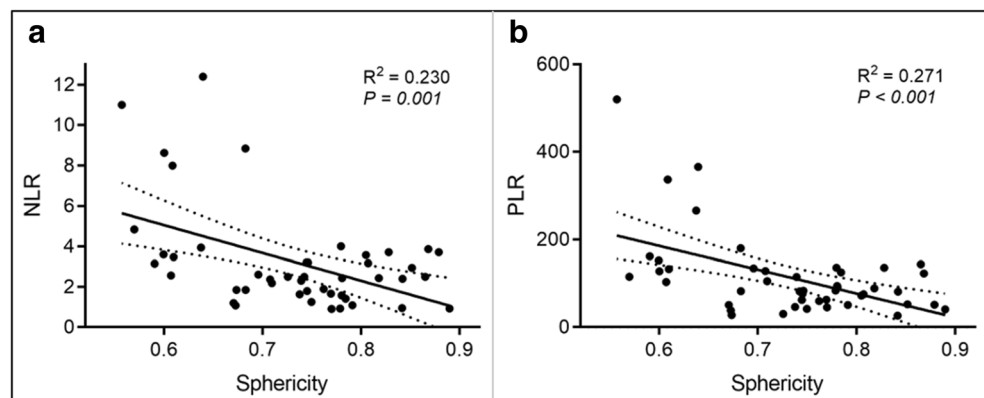
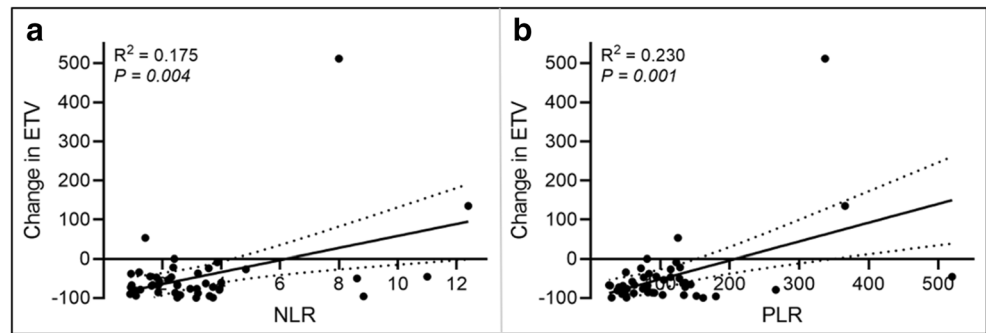


**Fig. 3** Linear regression of inflammatory markers and tumor response according to qEASL. This graph demonstrates that low (a) neutrophil-to-lymphocyte ratio (NLR) and (b) platelet-to-lymphocyte ratio (PLR) correlate with better tumor response according to quantitative European Association for the study of the Liver (qEASL) ( $p = 0.004$ ,  $p = 0.001$ )



independently associated with worse tumor response according to qEASL (Table 4). There was no significant difference in tumor response between patients treated with different DEB sizes (Table 2,  $p = 0.845$ ). CR, complete response; NLR, neutrophil-to-lymphocyte ratio; PLR, platelet-to-lymphocyte ratio; PR, partial response; qEASL, quantitative European Association for the Study of the Liver; SD, stable disease

### Correlation of baseline immunologic markers and progression-free survival after DEB-TACE

According to the multivariable Cox regression model, PFS was significantly reduced in patients with high NLR (hazard ratio = 1.31,  $p = 0.002$ , CI 1.10–1.56) or high PLR (hazard ratio = 1.013,  $p < 0.001$ , CI 1.01–1.02) when adjusted for TB and Child–Pugh class (Table 5).

When stratified according to mean NLR, low NLR was not associated with longer PFS ( $p = 0.075$ ). However, stratification according to mean PLR revealed significantly longer PFS

in patients with low PLR compared to patients with high PLR ( $p < 0.001$ ) (Fig. 5).

### Discussion

The main finding of this study is that quantitative immunologic biomarkers at baseline can predict volumetric enhancement-based tumor response to DEB-TACE and PFS in treatment-naïve patients with HCC. Additionally, systemic inflammation prior to treatment was associated with quantitative imaging features indicative of aggressive tumor growth.

Over the past decade, the complex nature of tumors and their reciprocal interactions with the surrounding TME have been increasingly recognized to be of critical importance for the regulation of carcinogenesis [12, 26]. As the majority of HCC develop in chronically inflamed cirrhotic livers, HCC is particularly remarkable with regard to the interaction of cancer cells with the immune system [27, 28]. The TME comprises a

**Fig. 4** Representative examples of HCC lesions with low (a) and high (b) tumor sphericity as assessed using radiomics feature analysis on baseline MRI. While low tumor sphericity indicative of extranodular and aggressive tumor growth (a) was associated with higher PLR, well-defined tumors with high sphericity (b) were associated with lower PLR. Additionally, patients with high PLR (a) revealed poorer tumor response after DEB-TACE (c, stable disease) as compared to patients with low PLR (d, partial response). White arrows indicate tumors

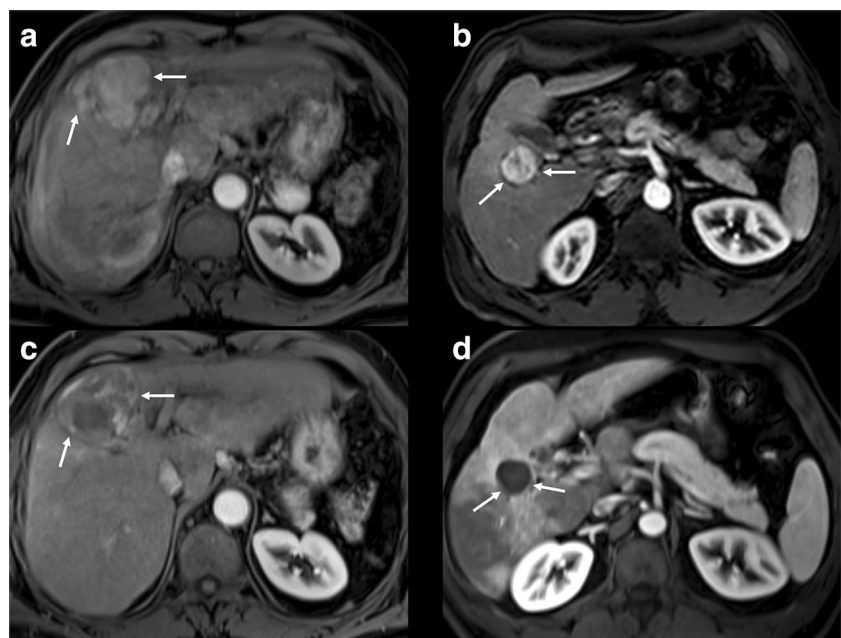


**Table 2** Comparison of patients with OR and non-OR regarding tumor features, lab values, BCLC stage, CP class, tumor location, and DEB sizes

		Non-OR (N= 19)	OR (N= 27)	p value
Tumor features	TTV	64.95 ± 88.16	33.54 ± 51.78	0.175
	ETV	37.85 ± 53.55	23.3 ± 25.55	0.282
	TB	3.80 ± 5.04	1.69 ± 2.12	0.099
	ETB	2.28 ± 3.20	1.21 ± 1.11	0.174
Lab values	WBC	6.17 ± 2.79	4.5 ± 1.92	0.02
	Platelet count	151.21 ± 74.44	89.96 ± 49.58	0.004
	ANC	3.89 ± 2.21	2.72 ± 1.35	0.03
	ALC	1.34 ± 0.86	1.23 ± 0.73	0.639
	NLR	4.14 ± 3.39	2.57 ± 1.56	0.072
	PLR	150.02 ± 121.88	87.12 ± 56.95	0.023
	AP	134.95 ± 78.29	124.48 ± 49.11 (N= 25)	0.59
	AST	49.89 ± 24.09	66.2 ± 50.19 (N= 25)	0.199
	ALT	38.63 ± 27.07	47.76 ± 27.29 (N= 25)	0.276
	Bilirubin (total)	0.87 ± 0.64	1.21 ± 0.82 (N= 25)	0.143
	AFP	4969.62 ± 15,485.83 (N= 13)	516.37 ± 1610.35 (N= 21)	0.322
	BCLC A/B+C+D	4/15	7/20	0.703
	CP A/B+C	13/6	15/12	0.379
	Tumor located in the right/left lobe	15/4	21/6	0.925
	DEB sizes 40–90, 70–150/100–300, 300–500 μm	10/9	15/12	0.845

AFP, alpha-fetoprotein; ALC, absolute lymphocyte count; ALT, alanine aminotransferase; ANC, absolute neutrophil count; AP, alkaline phosphatase; AST, aspartate aminotransferase; BCLC, Barcelona Clinic Liver Cancer; CP, Child-Pugh; DEB, drug-eluting bead; ETB, enhancing tumor burden; ETV, enhancing tumor volume; NLR, neutrophil-to-lymphocyte ratio; Non-OR, nonobjective response; OR, objective response; PLR, platelet-to-lymphocyte ratio; TB, tumor burden; TTV, total tumor volume; WBC, white blood count

set of specialized stromal cells including immune cell populations of variable composition and activity [29]. Specifically, chronic liver diseases are hypothesized to generate a pro-inflammatory milieu, which enables tumor formation and progression and potentially plays a critical role in the resistance of liver cancer cells to treatment [12–15]. Therefore, chronic inflammation and evasion from anti-tumoral immune response have been introduced as emerging hallmarks of cancer, which promote invasive tumor growth and foster several other hallmarks that ultimately contribute to a poor clinical outcome [26].

However, given the biological heterogeneity in HCC and its TME that hampers an accurate prognosis and treatment success, new biomarkers are needed that can measure the impact of the individual immune system activity on cancer growth patterns and susceptibility to loco-regional treatments.

Therefore, this study investigated the prognostic value of the baseline inflammatory ratios, NLR and PLR, measured in peripheral blood samples as biomarkers for clinical outcome after DEB-TACE. In particular, high NLR and PLR were predictive of worse volumetric enhancement-based tumor response ( $p = 0.014$  and  $p = 0.004$ ) and significantly shorter PFS after DEB-TACE ( $p = 0.002$  and  $p < 0.001$ ). Kaplan–Meier analysis revealed a cutoff value of mean PLR of 113.1, which significantly separates patients’ PFS stratified according to PLR ( $p = 0.001$ ). However, mean NLR did not achieve significant separation of the PFS curves ( $p = 0.477$ ).

Several studies have investigated the interaction between inflammation and tumor biology prior to treatment, trying to explain possible ways of immunosuppression based on the presence of neutrophils [30]. First, a high number of

**Table 3** Mean and median NLR and PLR per response category according to qEASL

	PD (N= 2)	SD (N= 17)	PR (N= 27)	CR
NLR	10.2 ± 3.11 (range 8–12.4)	3.42 ± 2.67 (median 2.37, range 0.93–11)	2.57 ± 1.56 (median 2.5, range 0.9–8.83)	–
PLR	351.57 ± 20.41 (range 337.14–366)	126.31 ± 104.93 (median 114.94, range 50.67–520)	87.12 ± 56.95 (median 75, range 26.32–266.2)	–

CR, complete response; NLR, neutrophil-to-lymphocyte ratio; PLR, platelet-to-lymphocyte ratio; PR, partial response; qEASL, quantitative European Association for the Study of the Liver; SD, stable disease

**Table 4** Three-step approach; this table shows the univariable and multivariable linear regression analysis of the association between NLR and PLR and tumor response according to qEASL, adjusting for Child–Pugh class, tumor burden, and alkaline phosphatase

	Univariable analysis <i>p</i> value	Multivariable analysis					
		Unstandardized coefficient beta	SE	Standardized coefficient beta	<i>p</i> value	95% CI	
<b>NLR</b>							
Child–Pugh class A vs B+C	0.1	−58.39	19.15	−0.31	0.004	−97.12	−19.66
TB (%)	0.001	7.39	2.62	0.29	0.008	2.09	12.70
AP (U/L)	<0.001	0.74	0.16	0.49	<0.001	0.42	1.05
NLR	0.003	9.98	3.86	0.27	0.014	2.17	17.80
<b>PLR</b>							
Child–Pugh class A vs B+C	0.1	−58.14	18.50	−0.31	0.003	−95.56	−20.73
TB	0.001	7.94	2.51	0.32	0.003	2.87	13.01
AP	<0.001	0.67	0.16	0.45	<0.001	0.35	0.99
PLR	0.001	0.32	0.10	0.32	0.004	0.11	0.53

AP, alkaline phosphatase; CI, confidence interval; NLR, neutrophil-to-lymphocyte ratio; PLR, platelet-to-lymphocyte ratio; qEASL, quantitative European Association for the Study of the Liver; SE, standard error; TB, tumor burden

neutrophils have been shown to suppress the activation and cytolytic anti-tumoral activity of lymphocytes and natural killer cells [31]. Second, secretion of VEGF by neutrophils in the peritumoral stroma of HCC was shown to promote neoangiogenesis, ultimately facilitating tumor growth [16]. Similar to neutrophils, high platelet count stimulates angiogenesis and tumor proliferation by enhanced secretion of growth factors including VEGF, platelet-derived growth factor, and platelet-derived serotonin [17, 32, 33].

Subsequently, it was shown that immunologic ratios such as NLR and PLR can be applied as predictors of microvascular invasion on histopathology [34–36]. These inflammatory markers have been previously reported to correlate with overall survival and tumor progression in various tumor entities [19, 35, 37]. In patients with HCC, inflammatory markers were correlated with tumor recurrence and overall survival after loco-regional therapy or liver transplant [18, 35, 38–43]. Liu et al showed that high NLR combined with aspartate aminotransferase-to-alanine aminotransferase ratio

was independently associated with worse overall survival in patients with HCC after TACE [38]. Moreover, Nicolini et al reported that PLR > 150 is an independent predictor of tumor recurrence after TACE [42]. Regarding other tumor entities, several studies showed that high PLR is associated with an increased rate of lymphodal metastases in colorectal and cervical cancer [44, 45]. On the contrary, tumor-infiltrating T lymphocytes can recognize tumor-associated antigens and trigger anti-tumor immune response [29]. Thus, T cell-inflamed tumors are commonly referred to as “hot tumors” that are more susceptible to immunomodulatory treatment compared to “cold” tumors without significant T cell infiltration [46]. While high lymphocyte counts are associated with a better prognosis and improved survival in HCC, low lymphocyte counts, in turn, are predictors of a poor clinical outcome, particularly if combined with high neutrophils or platelets [40, 42, 47]. One possible explanation for the positive prognostic effect of lymphocytes is that the infiltration of T lymphocytes in the TME may be secondary

**Table 5** Cox regression of NLR and PLR with the outcome of PFS, adjusting for Child–Pugh class and tumor burden

	<i>B</i>	SE	<i>p</i> value	Exp( <i>B</i> )	95% CI	
<b>NLR</b>						
Child–Pugh class A vs B+C	−0.69	0.41	0.09	0.50	0.23	1.11
TB	0.001	0.05	0.99	1.00	0.91	1.11
NLR	0.27	0.09	0.002	1.31	1.11	1.56
<b>PLR</b>						
Child–Pugh class A vs B+C	−0.61	0.41	0.135	0.54	0.24	1.21
TB	0.02	0.05	0.66	1.02	0.927	1.13
PLR	0.01	0.00	<0.001	1.01	1.01	1.02

CI, confidence interval; NLR, neutrophil-to-lymphocyte ratio; PFS, progression-free survival; PLR, platelet-to-lymphocyte ratio; SE, standard error; TB, tumor burden



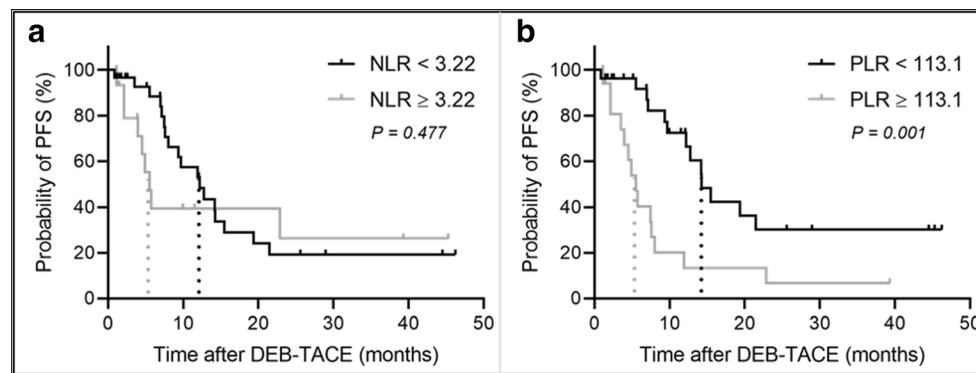


**Fig. 5** **a, b** Kaplan–Meier analysis of NLR and PLR with PFS. **a** Patients with low NLR (separated by the mean of 3.22) did not demonstrate significant longer PFS compared to patients with high NLR (12.17 and

5.51 months,  $p = 0.187$ ). **b** Patients with low PLR (< 113.1) showed longer PFS than patients with high PLR (15.5 and 5.51 months,  $p < 0.001$ ). Dotted lines indicate the median PFS of the respective group

due to tumor biology with lower ability for tumor progression [48]. In turn, the imbalance of high neutrophils or platelets with low lymphocyte count was significantly inversely associated with a single nodular tumor growth pattern on MRI in this study ( $p = 0.001$  and  $p < 0.001$ ), consistent with literature suggesting single nodular tumor growth being less aggressive with lower rates of metastases, portal vein invasion, and longer overall survival [49].

Innovations in anti-cancer strategies focus on immunotherapeutic interventions that aim at lowering the barrier of immunosuppression and restoring the resources of the immune system against cancer cells [13, 50]. Additionally, TACE has been investigated for its potential to affect the immunological response to the tumor in a possibly favorable way by systemically exposing tumor antigens to the immune system [51]. This may boost the local immune cell recruitment and infiltration in an otherwise immune-compromised TME, which built the basis for ongoing clinical trials to investigate potentially synergistic effects of TACE combined with immune checkpoint inhibitors (NCT03143270) [52, 53].

However, TACE-induced ischemia may also exacerbate tumor hypoxia and acidosis which hamper immune cell activity and may explain heterogeneous response rates to previously tested combination therapy regimens [54–57]. These mechanisms may ultimately represent a substantial clinical barrier for a broad and effective application of immunotherapies in liver cancer, both taken alone or in combination with TACE, making patient selection for such therapies a key issue.

Thus, there is currently a clinical need to develop reliable instruments for the functional characterization and live monitoring of the systemic immunological status prior to therapy to assess susceptibility and predict tumor response to loco-regional therapies [58]. Therefore, this study was tailored toward achieving a high level of clinical relevance and applicability by establishing the prognostic value of readily available laboratory markers to predict response to DEB-TACE and PFS in HCC. Additionally, the herein

tested laboratory biomarkers may help refine available staging systems and identify those HCC patients who will benefit from immuno-oncologic and loco-regional therapies such as TACE.

This study has some limitations. First, due to the retrospective design of the study, the number of patients was limited and a range of time points for image acquisition and laboratory values as well as various bead sizes were included. However, the impact of bead size on the clinical outcome was tested and did not show significant effects. In order to account for the prior limitations, the inclusion criteria were strictly defined and only treatment-naïve HCC was included into the analysis that was definitely diagnosed by histopathology or LI-RADS v2018 criteria. Although the majority of patients in this study was classified as BCLC B with maintained liver function, variability in TB and Child–Pugh class was accounted for by utilizing a multivariable linear regression model to assess the predictive value of immunological markers, which was adjusted for TB and Child–Pugh class. Due to the retrospective design of the study and thus small size of the cohort, the linear regression investigating the effect of the inflammatory ratios on tumor response (shown in Fig. 3) is weak and relies on few patients.

In conclusion, this study demonstrated the feasibility and validated the prognostic value of readily available immunologic scores for the prediction of volumetric enhancement-based tumor response and PFS after DEB-TACE. This set of biomarkers can easily be implemented in clinical practice providing a paradigm to guide and monitor the personalized application of loco-regional therapies with the ultimate goal of improving clinical outcome in HCC patients.

**Acknowledgments** We thank Luzie Dömel for her support and Claus Peter Nowak, M.Sc., for providing statistical advice. Dr. Savic is a participant in the BIH-Charité Junior Clinician Scientist Program funded by the Charité – Universitätsmedizin Berlin and the Berlin Institute of Health.

**Funding Information** The authors state that this work has not received any funding.

## Compliance with ethical standards

**Guarantor** The scientific guarantor of this publication is Julius Chapiro.

**Conflict of interest** The authors of this manuscript declare no relationships with any companies, whose products or services may be related to the subject matter of the article.

**Statistics and biometry** Claus Peter Nowak, M.Sc., from the Institute of Biometry and Clinical Epidemiology, Charité Berlin, kindly provided statistical advice for this manuscript.

**Informed consent** Written informed consent was waived by the Institutional Review Board.

**Ethical approval** Institutional Review Board approval was obtained.

### Methodology

- retrospective
- diagnostic or prognostic study
- performed at a single institution

## References

1. Bray F, Ferlay J, Soerjomataram I, Siegel RL, Torre LA, Jemal A (2018) Global cancer statistics 2018: GLOBOCAN estimates of incidence and mortality worldwide for 36 cancers in 185 countries. *CA Cancer J Clin* 68:394–424
2. Crissien AM, Frenette C (2014) Current management of hepatocellular carcinoma. *Gastroenterol Hepatol (N Y)* 10:153–161
3. Song JE, Kim DY (2017) Conventional vs drug-eluting beads transarterial chemoembolization for hepatocellular carcinoma. *World J Hepatol* 9:808–814
4. Baur J, Ritter CO, Germer CT, Klein I, Kickuth R, Steger U (2016) Transarterial chemoembolization with drug-eluting beads versus conventional transarterial chemoembolization in locally advanced hepatocellular carcinoma. *Hepat Med* 8:69–74
5. Dufour JF, Bargellini I, De Maria N, De Simone P, Goulis I, Marinho RT (2013) Intermediate hepatocellular carcinoma: current treatments and future perspectives. *Ann Oncol* 24(Suppl 2):ii24–ii29
6. European Association for the Study of the Liver, European Organisation for Research and Treatment of Cancer (2012) EASL-EORTC clinical practice guidelines: management of hepatocellular carcinoma. *J Hepatol* 56:908–943
7. Bruix J, Han KH, Gores G, Llovet JM, Mazzaferro V (2015) Liver cancer: approaching a personalized care. *J Hepatol* 62:S144–S156
8. Forner A, Reig M, Bruix J (2018) Hepatocellular carcinoma. *Lancet* 391:1301–1314
9. Bolondi L, Burroughs A, Dufour JF et al (2012) Heterogeneity of patients with intermediate (BCLC B) hepatocellular carcinoma: proposal for a subclassification to facilitate treatment decisions. *Semin Liver Dis* 32:348–359
10. Eisenhauer EA, Therasse P, Bogaerts J et al (2009) New response evaluation criteria in solid tumours: revised RECIST guideline (version 1.1). *Eur J Cancer* 45:228–247
11. Lambin P, Leijenaar RTH, Deist TM et al (2017) Radiomics: the bridge between medical imaging and personalized medicine. *Nat Rev Clin Oncol* 14:749–762
12. Roth GS, Decaens T (2017) Liver immunotolerance and hepatocellular carcinoma: patho-physiological mechanisms and therapeutic perspectives. *Eur J Cancer* 87:101–112
13. Prieto J, Melero I, Sangro B (2015) Immunological landscape and immunotherapy of hepatocellular carcinoma. *Nat Rev Gastroenterol Hepatol* 12:681–700
14. Coussens LM, Werb Z (2002) Inflammation and cancer. *Nature* 420:860–867
15. Unitt E, Rushbrook SM, Marshall A et al (2005) Compromised lymphocytes infiltrate hepatocellular carcinoma: the role of T-regulatory cells. *Hepatology* 41:722–730
16. Kuang DM, Zhao Q, Wu Y et al (2011) Peritumoral neutrophils link inflammatory response to disease progression by fostering angiogenesis in hepatocellular carcinoma. *J Hepatol* 54:948–955
17. Bambace NM, Holmes CE (2011) The platelet contribution to cancer progression. *J Thromb Haemost* 9:237–249
18. Zhou DS, Xu L, Luo YL et al (2015) Inflammation scores predict survival for hepatitis B virus-related hepatocellular carcinoma patients after transarterial chemoembolization. *World J Gastroenterol* 21:5582–5590
19. Zheng J, Cai J, Li H et al (2017) Neutrophil to lymphocyte ratio and platelet to lymphocyte ratio as prognostic predictors for hepatocellular carcinoma patients with various treatments: a meta-analysis and systematic review. *Cell Physiol Biochem* 44:967–981
20. American College of Radiology (2018) American College of Radiology: liver imaging reporting and data system. American College of Radiology, Virginia Available via <https://www.acr.org/Clinical-Resources/Reporting-and-Data-Systems/LI-RADS/CT-MRI-LI-RADS-v2018>. Accessed 7 Feb 2020
21. Tacher V, Lin M, Duran R et al (2016) Comparison of existing response criteria in patients with hepatocellular carcinoma treated with transarterial chemoembolization using a 3D quantitative approach. *Radiology* 278:275–284
22. van Griethuysen JJM, Fedorov A, Parmar C et al (2017) Computational radiomics system to decode the radiographic phenotype. *Cancer Res* 77:e104–e107
23. Heinze G, Wallisch C, Dunkler D (2018) Variable selection - a review and recommendations for the practicing statistician. *Biom J* 60:431–449
24. Kim HC, Suk KT, Kim DJ et al (2014) Transarterial chemoembolization in Barcelona Clinic Liver Cancer stage 0/A hepatocellular carcinoma. *World J Gastroenterol* 20:745–754
25. Nelen SD, Verhoeven RHA, Lemmens VEPP, de Wilt JHW, Bosscha K (2017) Increasing survival gap between young and elderly gastric cancer patients. *Gastric Cancer* 20:919–928
26. Hanahan D, Weinberg RA (2011) Hallmarks of cancer: the next generation. *Cell* 144:646–674
27. Buonaguro L, Tagliamonte M, Petrizzo A, Damiano E, Tornesello ML, Buonaguro FM (2015) Cellular prognostic markers in hepatocellular carcinoma. *Future Oncol* 11:1591–1598
28. O'Rourke JM, Sagar VM, Shah T, Shetty S (2018) Carcinogenesis on the background of liver fibrosis: implications for the management of hepatocellular cancer. *World J Gastroenterol* 24:4436–4447
29. Gajewski TF, Schreiber H, Fu YX (2013) Innate and adaptive immune cells in the tumor microenvironment. *Nat Immunol* 14:1014–1022
30. Rai V, Abdo J, Alsuwaidan AN, Agrawal S, Sharma P, Agrawal DK (2018) Cellular and molecular targets for the immunotherapy of hepatocellular carcinoma. *Mol Cell Biochem* 437:13–36
31. Mantovani A (2009) The yin-yang of tumor-associated neutrophils. *Cancer Cell* 16:173–174
32. Sarrouilhe D, Clarhaut J, Defamie N, Mesnil M (2015) Serotonin and cancer: what is the link? *Curr Mol Med* 15:62–77
33. Nieswandt B, Hafner M, Echtenacher B, Mannel DN (1999) Lysis of tumor cells by natural killer cells in mice is impeded by platelets. *Cancer Res* 59:1295–1300
34. Rungsakulkij N, Mingphruedhi S, Suragul W, Tangtawee P, Muangkaew P, Aeesoa S (2018) Platelet-to-lymphocyte ratio and

- large tumor size predict microvascular invasion after resection for hepatocellular carcinoma. *Asian Pac J Cancer Prev* 19:3435–3441
35. Zheng J, Seier K, Gonen M et al (2017) Utility of serum inflammatory markers for predicting microvascular invasion and survival for patients with hepatocellular carcinoma. *Ann Surg Oncol* 24:3706–3714
  36. Yu Y, Song J, Zhang R et al (2017) Preoperative neutrophil-to-lymphocyte ratio and tumor-related factors to predict microvascular invasion in patients with hepatocellular carcinoma. *Oncotarget* 8:79722–79730
  37. Wu J, Chen M, Liang C, Su W (2017) Prognostic value of the pretreatment neutrophil-to-lymphocyte ratio in cervical cancer: a meta-analysis and systematic review. *Oncotarget* 8:13400–13412
  38. Liu C, Jia BS, Zou BW et al (2017) Neutrophil-to-lymphocyte and aspartate-to-alanine aminotransferase ratios predict hepatocellular carcinoma prognosis after transarterial embolization. *Medicine (Baltimore)* 96:e8512
  39. Xiao WK, Chen D, Li SQ, Fu SJ, Peng BG, Liang LJ (2014) Prognostic significance of neutrophil-lymphocyte ratio in hepatocellular carcinoma: a meta-analysis. *BMC Cancer* 14:117
  40. Xue TC, Jia QA, Ge NL et al (2015) The platelet-to-lymphocyte ratio predicts poor survival in patients with huge hepatocellular carcinoma that received transarterial chemoembolization. *Tumour Biol* 36:6045–6051
  41. Sullivan KM, Groeschl RT, Turaga KK et al (2014) Neutrophil-to-lymphocyte ratio as a predictor of outcomes for patients with hepatocellular carcinoma: a Western perspective. *J Surg Oncol* 109:95–97
  42. Nicolini D, Agostini A, Montalti R et al (2017) Radiological response and inflammation scores predict tumour recurrence in patients treated with transarterial chemoembolization before liver transplantation. *World J Gastroenterol* 23:3690–3701
  43. Liu C, Li L, Lu WS et al (2018) A novel combined systemic inflammation-based score can predict survival of intermediate-to-advanced hepatocellular carcinoma patients undergoing transarterial chemoembolization. *BMC Cancer* 18:216
  44. Kwon HC, Kim SH, Oh SY et al (2012) Clinical significance of preoperative neutrophil-lymphocyte versus platelet-lymphocyte ratio in patients with operable colorectal cancer. *Biomarkers* 17:216–222
  45. Wang D, Wu M, Feng FZ et al (2013) Pretreatment neutrophil-to-lymphocyte and platelet-to-lymphocyte ratios do not predict survival in patients with cervical cancer treated with neoadjuvant chemotherapy and radical hysterectomy. *Chin Med J (Engl)* 126:1464–1468
  46. van der Woude LL, Gorrís MAJ, Halilovic A, Figdor CG, de Vries IJM (2017) Migrating into the tumor: a roadmap for T cells. *Trends Cancer* 3:797–808
  47. Motomura T, Shirabe K, Mano Y et al (2013) Neutrophil-lymphocyte ratio reflects hepatocellular carcinoma recurrence after liver transplantation via inflammatory microenvironment. *J Hepatol* 58:58–64
  48. Pufnock JS, Rothstein JL (2009) Oncoprotein signaling mediates tumor-specific inflammation and enhances tumor progression. *J Immunol* 182:5498–5506
  49. Shimada M, Rikimaru T, Hamatsu T et al (2001) The role of macroscopic classification in nodular-type hepatocellular carcinoma. *Am J Surg* 182:177–182
  50. Harding JJ, El Dika I, Abou-Alfa GK (2016) Immunotherapy in hepatocellular carcinoma: primed to make a difference? *Cancer* 122:367–377
  51. Xue TC, Jia QA, Ge NL, Chen Y, Zhang BH, Ye SL (2015) Imbalance in systemic inflammation and immune response following transarterial chemoembolization potentially increases metastatic risk in huge hepatocellular carcinoma. *Tumour Biol* 36:8797–8803
  52. Li F, Guo Z, Lizee G, Yu H, Wang H, Si T (2014) Clinical prognostic value of CD4+CD25+FOXP3+regulatory T cells in peripheral blood of Barcelona Clinic Liver Cancer (BCLC) stage B hepatocellular carcinoma patients. *Clin Chem Lab Med* 52:1357–1365
  53. Mizukoshi E, Nakamoto Y, Arai K et al (2011) Comparative analysis of various tumor-associated antigen-specific T-cell responses in patients with hepatocellular carcinoma. *Hepatology* 53:1206–1216
  54. Jia ZZ, Jiang GM, Feng YL (2011) Serum HIF-1 $\alpha$  and VEGF levels pre- and post-TACE in patients with primary liver cancer. *Chin Med Sci J* 26:158–162
  55. Warburg O, Gawehn K, Geissler AW (1960) The transformation of embryonal metabolism in cancer metabolism. *Z Naturforsch B* 15B:378–379
  56. Semaan A, Dietrich D, Bergheim D et al (2017) CXCL12 expression and PD-L1 expression serve as prognostic biomarkers in HCC and are induced by hypoxia. *Virchows Arch* 470:185–196
  57. Zhou ZQ, Tong DN, Guan J et al (2016) Follicular helper T cell exhaustion induced by PD-L1 expression in hepatocellular carcinoma results in impaired cytokine expression and B cell help, and is associated with advanced tumor stages. *Am J Transl Res* 8:2926–2936
  58. Schreiber RD, Old LJ, Smyth MJ (2011) Cancer immunoeediting: integrating immunity's roles in cancer suppression and promotion. *Science* 331:1565–1570

**Publisher's note** Springer Nature remains neutral with regard to jurisdictional claims in published maps and institutional affiliations.